Circulation
Cardiovascular Imaging

Multifactorial Relationship Between ^{18}F-Fluoro-Deoxy-Glucose Positron Emission Tomography Signaling and Biomechanical Properties in Unruptured Aortic Aneurysms

Alain Nchimi, Jean-Paul Cheramy-Bien, T. Christian Gasser, Gauthier Namur, Pierre Gomez, Laurence Seidel, Adelin Albert, Jean-Olivier Defraigne, Nicos Labropoulos and Natzi Sakalihasan

Circ Cardiovasc Imaging. 2014;7:82-91; originally published online November 4, 2013;
doi: 10.1161/CIRCIMAGING.112.000415
Circulation: Cardiovascular Imaging is published by the American Heart Association, 7272 Greenville Avenue, Dallas, TX 75231

Print ISSN: 1941-9651. Online ISSN: 1942-0080

Multifactorial Relationship Between ^{18}F-Fluoro-Deoxy-Glucose Positron Emission Tomography Signaling and Biomechanical Properties in Unruptured Aortic Aneurysms

Alain Nchimi, MD; Jean-Paul Cheramy-Bien, MLT; T. Christian Gasser, PhD; Gauthier Namur, MD; Pierre Gomez, MD; Laurence Seidel, MSc; Adelin Albert, PhD; Jean-Olivier Defraigne, MD, PhD; Nicos Labropoulos, MD, PhD; Natzi Sakalihasan, MD, PhD

Background—The relationship between biomechanical properties and biological activities in aortic aneurysms was investigated with finite element simulations and ^{18}F-fluoro-deoxy-glucose (^{18}F-FDG) positron emission tomography.

Methods and Results—The study included 53 patients (45 men) with aortic aneurysms, 47 infrarenal (abdominal aortic) and 6 thoracic (thoracic aortic), who had ≥1 ^{18}F-FDG positron emission tomography/computed tomography. During a 30-month period, more clinical events occurred in patients with increased ^{18}F-FDG uptake on their last examination than in those without (5 of 18 [28%] versus 2 of 35 [6%]; P=0.03). Wall stress and stress/strength index computed by finite element simulations and ^{18}F-FDG uptake were evaluated in a total of 68 examinations. Twenty-five (38%) examinations demonstrated ≥1 aneurysm wall area of increased ^{18}F-FDG uptake. The mean number of these areas per examination was 1.6 (18 of 11) in thoracic aortic aneurysms versus 0.25 (14 of 57) in abdominal aortic aneurysms, whereas the mean number of increased uptake areas colocalizing with highest wall stress and stress/strength index areas was 0.55 (6 of 11) and 0.02 (1 of 57), respectively. Quantitatively, ^{18}F-FDG positron emission tomographic uptake correlated positively with both wall stress and stress/strength index (P<0.05). ^{18}F-FDG uptake was particularly high in subjects with personal history of angina pectoris and familial aneurysm.

Conclusions—Increased ^{18}F-FDG positron emission tomographic uptake in aortic aneurysms is strongly related to aneurysm location, wall stress as derived by finite element simulations, and patient risk factors such as acquired and inherited susceptibilities. **(*Circ Cardiovasc Imaging*. 2014;7:82-91.)**

Key Words: aneurysm ■ aorta ■ tomography

Aneurysms are permanent vascular dilatations that involve the aorta in ≤10% of subjects >65 years of age, with more than half localized in the infrarenal aorta.[1,2] Their rupture causes death in ≤90% of cases,[2,3] and according to recent trials, the operative mortality does not exceed 5%.[4] The aneurysm maximal diameter identifies the time point when the risk of rupture exceeds that of repair, hence indicating a preventive intervention in asymptomatic patients.[5–7] Research, however, has been driven toward more patient-specific risk assessment because aneurysms above the critical diameter thresholds may never rupture, whereas smaller aneurysms will.[8–10]

Clinical Perspective on p 91

Rupture occurs when the wall stress exceeds the wall strength. Aortic geometry can be used for finite element simulations (FES)[11,12] providing, among other estimates, wall stress. Before rupture occurs, wall stress is involved in aneurysmal expansion and remodeling; the latter triggers and amplifies numerous biological mechanisms that may result in apposition of an intraluminal thrombus with its own biomechanical[13] and biological characteristics.[14–17] The biological activity of the aortic wall can be evaluated indirectly through energy consumption using ^{18}F-fluoro-deoxy-glucose (^{18}F-FDG) as a tracer for positron emission tomographic (PET) imaging.[18] ^{18}F-FDG uptake is not uncommon in aortic aneurysms[19,20] and has been shown to correlate with the amount of inflammatory cells, proteolytic activity, and risk of rupture.[21–23] Xu et al[24] previously evidenced associations among biological activity, wall stress estimates, and rupture in 3 patients with aortic aneurysms. The actual relationship between biomechanical parameters and biological activity, however, has never been studied in large series.

Our study was designed to assess the relationship and the independent determinants between biomechanical estimates of wall stress and ^{18}F-FDG uptake in unruptured aortic aneurysms.

Received November 28, 2012; accepted October 16, 2013.

From the Departments of Cardiovascular and Thoracic Imaging (A.N.) and Cardiovascular and Thoracic Surgery (J.-P.C.-B., J.O.D., N.S.), University Hospital, Liège, Belgium; Department of Solid Mechanics, Royal Institute of Technology (KTH), Stockholm, Sweden (T.C.G.); Department of Nuclear Medicine, Centre Hospitalier Chrétien St Joseph, Liège, Belgium (G.N., P.G.); Medical Informatics and Biostatistics, University of Liège, Liège, Belgium (L.S., A.A.); and Stony Brook University Medical Center, NY (N.L.).

The Data Supplement is available at http://circimaging.ahajournals.org/lookup/suppl/doi:10.1161/CIRCIMAGING.112.000415/-/DC1.

Correspondence to Alain Nchimi, MD, Department of Cardiovascular and Thoracic Imaging, University Hospital Sart Tilman B35, Liège 4000, Belgium. E-mail anchimi@chu.ulg.ac.be

Methods

Study Patients

This study is part of a larger trial aiming to determine the role of ^{18}F-FDG PET in aortic aneurysm rupture risk assessment as approved by the institutional review board.[25] It included 53 patients (45 men) with aortic aneurysm who underwent ≥1 whole-body ^{18}F-FDG PET examination using contrast-enhanced computed tomography (CT) for attenuation correction in a single center within a 5-year period. All patients provided written informed consent. Patients with aneurysm of the ascending thoracic aorta were excluded to avoid pathophysiology clustering. There were 47 patients with aneurysms involving the infrarenal aorta (abdominal aortic aneurysm [AAA]) and 6 the thoracic aorta (thoracic aortic aneurysm [TAA]), including arch (n=1), descending thoracic aorta (n=2), and thoracoabdominal aortic aneurysms, with the largest diameter at the level of the thoracic aorta (n=3). Between 1 and 5 ^{18}F-FDG PET examinations were performed on 44, 6, 1, 1, and 1 patients, respectively, resulting in a total of 68 examinations (11 in TAAs and 57 in AAAs). The average interscan duration among patients was 7.2±5.9 months. Based on clinical and imaging follow-up, significant events related to the aortic disease were defined as an aneurysm growth of >1 cm per year, dissection, rupture, or emergency surgery. ^{18}F-FDG PET CT and FES imaging data acquisition procedures are detailed in Method I in the Data Supplement.

Visual Image Analysis

Experts with ≥6 years of experience in nuclear imaging examined all 68 tests. Increased ^{18}F-FDG uptake in the aortic aneurysm wall was documented by identifying any area with >1 cm of increased signaling compared with the intra-arterial background and distant aortic wall segments. Examinations were declared positive when ≥1 such area was noted. Clinical reports were also carefully analyzed to describe ^{18}F-FDG uptake as diffuse, monofocal, or plurifocal and to identify and localize uptake areas on the corresponding CT images using predefined anatomic landmarks. Specifically, this required the readers to identify the center of the area relative to a vascular or a vertebral landmark cranio-caudally and then to localize the main quadrant of the area relative to sagittal and coronal lines across the aortic center.

In a second step, a radiologist with >5 years of experience in vascular imaging analyzed the 68 examinations by the FES method using the A4clinics software system (VASCOPS GmbH; Graz, Austria)[26] set on read-only mode that did not allow any modification of the aortic segmentation and geometry. The radiologist determined the maximal

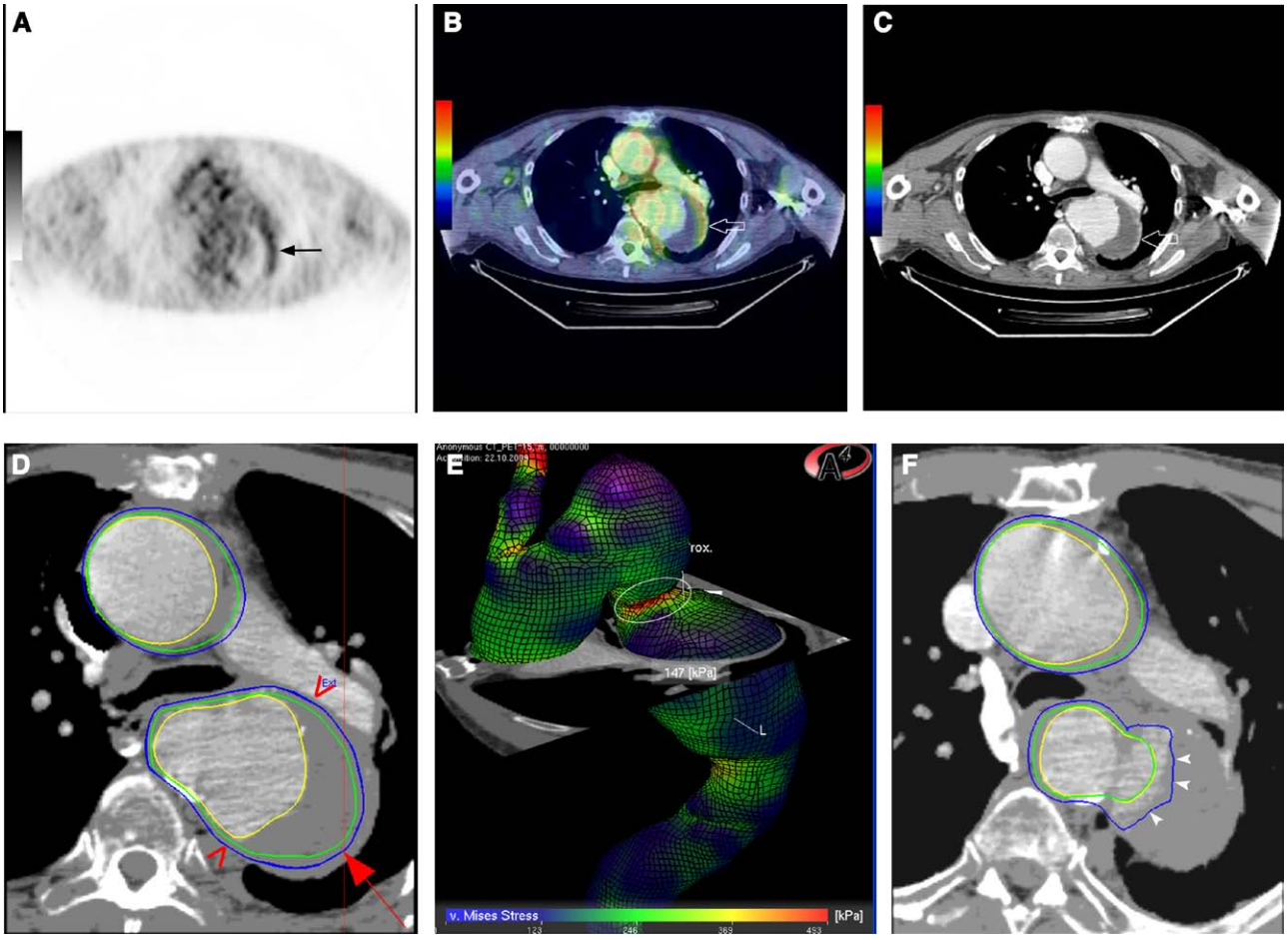

Figure 1. ^{18}F-fluoro-deoxy-glucose (^{18}F-FDG) uptake and wall stress estimates in a 79-year-old man with a descending thoracic aortic aneurysm. An area of increased ^{18}F-FDG uptake (arrows) is identified on axial positron emission tomographic (PET; **A**), fused PET computed tomographic (CT; **B**), and then on CT (**C**) images. Reconstruction of a model using CT image, magnified at the same level (red arrow, **D**), including external and luminal aortic boundaries (blue and yellow lines) and hypothetical wall limit paralleling the external contour (green line), allows diameter (between brackets) and thrombus (between yellow and green lines) assessment. **E**, Color-coded 3-dimensional wall stress map of the aorta after pressurization of this model, where the axial slice in the area of interest has been inserted, showing the wall stress estimate (147 kPa). By convention, color code represents intensity scale ranging from deep blue to red. An artifact located >1 cm proximally in the aorta, exhibiting a red spot of increased wall stress (**E**, circled area), is excluded for analysis and explained in **F** by failure of the aortic contour reconstruction (arrowheads on blue line). The patient denied surgery and experienced acute dissection 5 months after this examination. The intimal tear was located around previously increased ^{18}F-FDG uptake area. The patient eventually died 1 week after this complication.

Table 1. Patient Demographics and Risk Factors for Aortic Aneurysms (n=53)

Patient Characteristic	n (%)	Mean±SD
Age, y		72.0±8.2
Sex (male)	45 (85)	
Current smoking	24 (45)	
Stopped smoking	19 (36)	
Aneurysm location (TAA)	6 (11)	
Other arterial aneurysms	13 (24)	
Diabetes mellitus	11 (21)	
Arterial hypertension	32 (60)	
Dyslipidemia*	36 (69)	
COPD	15 (28)	
Stroke	9 (17)	
Peripheral artery disease	20 (38)	
Angina pectoris	15 (28)	
Renal insufficiency†	8 (15)	
Acute myocardial infarction	22 (41)	
Familial aneurysm	6 (12)	
Follow-up duration, mo		11.4±8.6
Adverse event	7 (13)	

COPD indicates chronic obstructive pulmonary disease; and TAA, descending thoracic aortic aneurysm.

*Increased serum levels of triglycerides, low-density lipoprotein cholesterol, or both

†Clearance of creatinine <60 mL/min.

values of wall stress, stress/strength index, and thrombus thickness in all 68 examinations. The same radiologist verified whether the area containing the highest values of either wall stress or stress/strength index estimates colocalized with an area of increased ^{18}F-FDG uptake as described in the clinical reports. For visual analyses, maximal wall stress and stress/strength index were expressed as relative intensity in areas with ^{18}F-FDG uptake to compensate for interpatient variability (Method II in the Data Supplement).

Quantitative Image Analysis

Two other observers with >5 years of experience in vascular imaging and vascular surgery, respectively, were asked to determine in consensus the areas of interest for the quantitative analysis and the topographical correspondences between wall stress and ^{18}F-FDG PET. Multiplanar and volumetric analyses of CT, ^{18}F-FDG PET, and fused ^{18}F-FDG PET/CT images (all had similar spatial coordinates) were performed on a dedicated workstation (Advantage Windows, release 4.3; GE Healthcare).

^{18}F-Fluoro-Deoxy-Glucose PET

On CT images, a volume of interest (VOI) was automatically selected to include the aorta using the high intravascular attenuation (mean, 214 [range, 70–335] Hounsfield units). Structures that were included in the volume because of similar attenuation values were manually deleted, and the remaining VOI was copied and pasted on ^{18}F-FDG PET images. If needed (eg, because of a slight patient position change between CT and PET images), the pasted VOI was slightly adjusted to include the whole intraluminal thrombus and match the anatomic contours. Then, the mean and SD of the ^{18}F-FDG uptake in the VOI were estimated quantitatively using standardized uptake value (SUV) as shown in Method III in the Data Supplement. Within this VOI, the observers selected all clusters of >10 voxels with SUV above the threshold of mean+2SD of the whole volume. Using fused ^{18}F-FDG PET-CT images, they excluded the areas belonging to structures surrounding the aorta (eg, vertebra, ureter, duodenum; n=7) or to the aortic lumen (n=19). Another VOI was drawn manually to include the right hepatic lobe and the retrohepatic inferior vena cava and to determine their maximal SUVs. Then, to compensate for contrast-enhanced CT overcorrection and patient variability, the aortic wall maximal SUVs were normalized as SUV-to-liver (SUV_{RL}) and SUV-to-venous background (SUV_{RV}) ratios.

Finite Element Simulations

FES image displays (A4clinics) were set to highlight clusters of >10 elements exhibiting values of wall stress and stress/strength index estimates of ≥mean of whole aorta+2SD. The geometry of these areas was checked on CT to exclude reconstruction failures (n=20; eg, complex geometry, kinking, bifurcations), as shown in Figure 1.

Topographical Matching of ^{18}F-FDG PET and FES

In all selected areas, intraluminal thrombus thickness, aortic diameter, and maximal values of SUV_{RL}, SUV_{RV}, wall stress, and stress/strength index were recorded. Each observer instructed the other to derive ^{18}F-FDG uptake and FES estimates on selected areas. The areas were topographically matched using CT images, with the rule that any part of one intersects the other by ≤1 cm to its center (Figure 1).

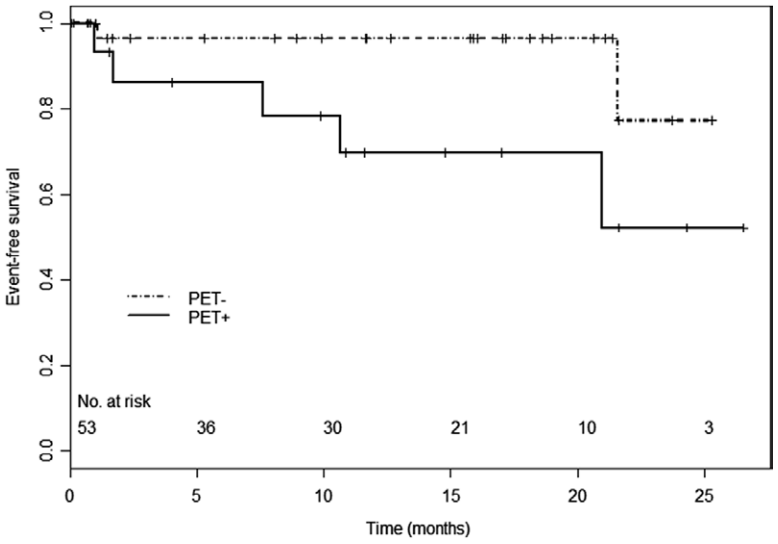

Figure 2. Thirty-month event-free survival curves in positron emission tomography (PET)–positive and PET-negative patients according to increased ^{18}F-fluoro-deoxy-glucose uptake at the last examination.

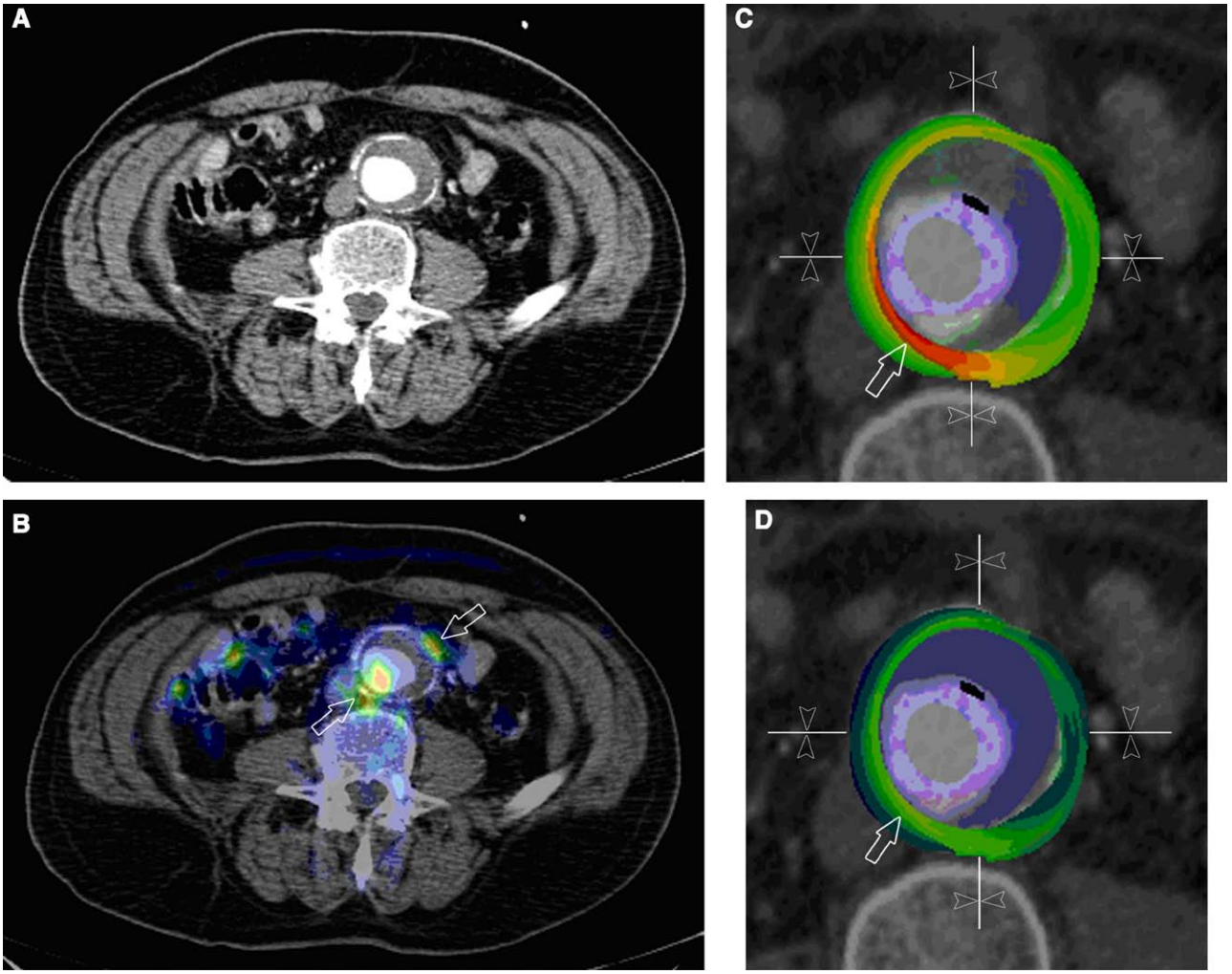

Figure 3. Partial coincidence between positron emission tomographic (PET) imaging findings and finite element simulation (FES) estimates in an 80-year-old man with abdominal aortic aneurysm (**A**). After fusion with ^{18}F-fluoro-deoxy-glucose (^{18}F-FDG) PET imaging (**B**), 2 distinct aortic areas of ^{18}F-FDG uptake are seen (arrows): one in the left anterior and the other in the right posterior quadrants. On FES, these areas show, respectively, average and increased (arrows) wall stress (**C**; wall stress=161 kPa) and stress/strength index (**D**; stress/strength index=0.34). By convention, color code represents intensity scale ranging from deep blue to red. The patient's last follow-up computed tomography showed no aneurysm enlargement after 1 year. He eventually died shortly after from lung cancer.

Statistical Methods

Statistics were mainly descriptive. Quantitative data were summarized by mean and SD, whereas numbers and percentages were used for categorical findings. Correlations were calculated to assess the relationships between SUV_{RL} and SUV_{RV} values and the corresponding wall stress and stress/strength index estimates. Event-free survival curves were compared using the log-rank test. The general linear mixed model, which accounts for repeated measurements within subjects, was used to compare AAAs versus TAAs with respect to imaging and FES in areas of interest and to assess the relationship between SUV_{RV} and biomechanical parameters, aneurysm location, and patient-specific factors. Results were significant at the 5% critical level (P<0.05). All statistical calculations were performed with SAS (version 9.3 for Windows).

Results

Patient Characteristics

Patient characteristics are described in Table 1. Five of the 6 patients (83%) with TAA were above the rupture risk threshold of 55 mm, whereas only 24 of the 47 patients (51%) with AAA were higher than the corresponding 50-mm threshold. During the follow-up period, adverse clinical events occurred in 7 (13%) patients. The outcomes of all patients after the last examination with regard to ^{18}F-FDG PET uptake and colocalization with maximal FES estimates are given in Table I in the Data Supplement. Among the 53 patients, 18 (34%) were ^{18}F-FDG PET positive (ie, with increased ^{18}F-FDG uptake on their last examination), and 35 were ^{18}F-FDG PET negative. The proportion of clinical events was higher (28% versus 6%; P=0.03), and the 30-month event-free survival was worse in the former group (log-rank test: P=0.040; Figure 2).

Visual Analyses at Segment Level

Among the 68 ^{18}F-FDG PET examinations, there were 25 (38%) with visually increased aortic uptake. These uptakes were diffuse, monofocal, bifocal, and trifocal, respectively, in 1, 18, 5, and 1 examinations, yielding a total of 32 areas. Of these areas, 18 (56%) were in TAAs and 14 (44%) in AAAs. For wall stress, the mean relative intensity was 55±45% for all examinations (76±38% in TAAs versus 31±41% in AAAs).

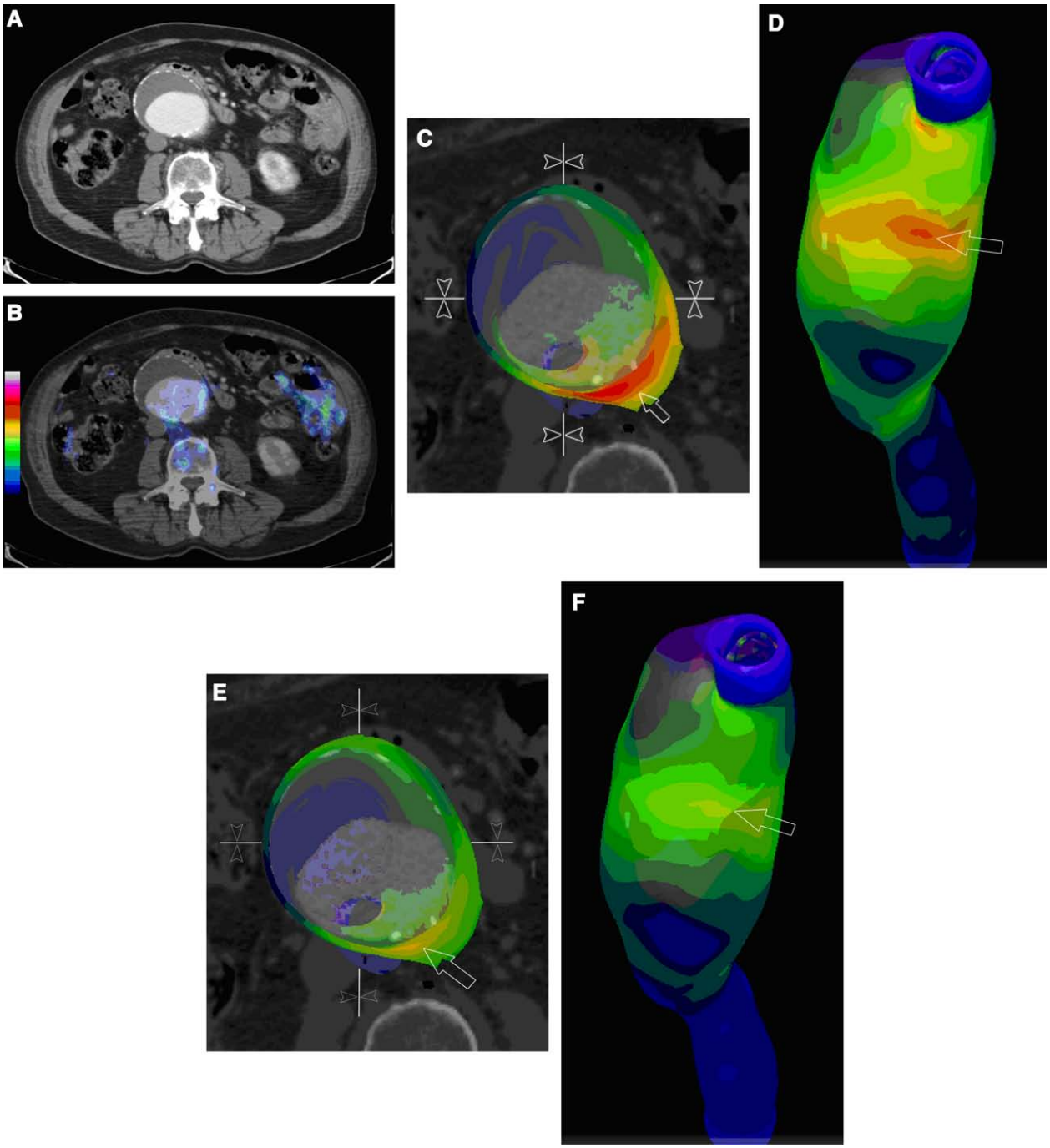

Figure 4. Absence of coincidence between positron emission tomographic (PET) imaging findings and finite element simulation estimates in a 72-year-old man with abdominal aortic aneurysm (**A**). After fusion with ^{18}F-fluoro-deoxy-glucose (^{18}F-FDG) PET imaging (**B**), no area of ^{18}F-FDG uptake is seen, whereas coronal and axial projections of the aortic geometry show a large area (arrows) of increased wall stress (**C** and **D**; wall stress=315 kPa) and stress/strength index (**E** and **F**; stress/strength index=0.75) in the left posterior quadrant of the aorta. By convention, color code represents intensity scale ranging from deep blue to red. The patient's aneurysm was surgically repaired without delay because of the aneurysm diameter.

The stress/strength index equaled 57±48% for all examinations (77±37% in TAAs versus 33±49% in AAAs). The mean number of uptake areas per examination was 1.6 (18 of 11) in TAAs versus 0.25 (14 of 57) in AAAs, whereas the mean number of uptake areas colocalizing with highest wall stress and stress/strength index areas was, respectively, 0.55 (6 of 11) in TAAs and 0.02 (1 of 57) in AAAs. Examples for PET imaging findings and FES estimates are shown in Figures 3 and 4.

Quantitative Analyses

On the entire set of examinations, 163 areas were selected: 54 areas based on ^{18}F-FDG PET (mean: 1.46±0.69 areas per patient) and 109 on FES (mean: 1.85±0.85 areas per patient; P=0.0019). Wall stress (P=0.017) and wall stress/strength index (P=0.011) estimates were significantly higher in TAAs than in AAAs, unlike SUV_{RL} (P=0.068), SUV_{RV} (P=0.12), local aortic diameter (P=0.21), and thrombus thickness

Table 2. Values of Selected Areas of ^{18}F-FDG Uptake, FES Estimates, Aortic Diameter, and Thrombus Thickness According to the Aneurysm Location

Variable	AAA n=131 Areas	TAA n=32 Areas	*P* Value*
SUV_{RL}	0.68±0.15	0.86±0.24	0.068
SUV_{RV}	1.22±0.28	1.53±0.46	0.12
Wall stress, kPa	174±60.5	320±161	0.017
Stress/strength index	0.38±0.15	0.81±0.33	0.011
Local diameter, mm	42.6±10.3	47.3±19.0	0.21
Thrombus thickness, mm	2.01±2.08	2.53±3.74	0.39

AAA indicates abdominal aortic aneurysm; ^{18}F-FDG, ^{18}F-fluoro-deoxy-glucose; FES, finite element simulation; SUV_{RL}, standardized uptake value-to-liver; SUV_{RV}, standardized uptake value-to-venous background; and TAA, descending thoracic aortic aneurysm.

*Adjusted for repeated values within subjects.

(*P*=0.39; Table 2). A strong correlation (*r*=0.71; *P*<0.0001) was found between SUV_{RL} and SUV_{RV} (Figure 5). Positive correlations were observed between ^{18}F-FDG uptake and both wall stress and stress/strength index (Figures 6 and 7), but these were lower in FES-selected areas (*r*=0.28 for wall stress and *r*=0.30 for stress/strength index) than in ^{18}F-FDG PET-selected areas (*r*=0.36 for wall stress and *r*=0.37 for wall stress/strength index using SUV_{RV}, and *r*=0.44 for both wall stress and wall stress/strength index using SUV_{RL}; all *P*<0.05).

A general linear mixed model was fitted to SUV_{RV} values to assess potential associations with FES-related characteristics and patient-related risk factors while accounting for repeated scans within patients (Table 3). As a result, SUV_{RV} values were significantly higher in TAA- than in AAA-selected areas (*P*=0.027) in subjects with a personal history of angina pectoris (*P*=0.012) and in patients with familial aneurysm (*P*=0.0065); no other parameter was significant.

Discussion

There are only a few case studies in the literature that correlate wall stress estimates to ^{18}F-FDG uptake, often with opposite findings.[24,27] In the present hypothesis-generating work, we first evaluated such correlations visually and patient outcome. We observed differences between TAAs and AAAs on both the properties of imaging techniques and their rates of colocalization. This may be because of known structural differences between TAAs and AAAs: a larger intraluminal thrombus is a well-documented characteristic of AAA. However, inclusion of follow-up examinations, even after TAA dissection and false lumen thrombosis, did not support this explanation but, to the contrary, caused a larger dispersion of thrombus thickness in TAAs than in AAAs (2.53±3.74 versus 2.01±2.08 mm). However, the wall strength is better anticipated in the absence of extensive calcifications[28] or large intraluminal thrombus such as in AAAs.[15,29–31] Despite this, only minor differences were observed between the magnitudes of wall stress and stress/strength index, meaning that FES estimates were actually largely weighted by wall stress compared with wall strength. Therefore, further adjustments in wall strength assumptions are needed to increase correlations between ^{18}F-FDG uptake and stress/strength index, especially in AAAs.

When it comes to outcome prediction, Fillinger et al[32] and Sakalihasan et al[21] first suggested that wall stress estimates and ^{18}F-FDG uptake may perform better than the maximal aneurysm diameter. It is unknown whether biomechanical stress generates biological activity or, inversely, but the 2 imaging methods assess the pathophysiological activities involved in aneurysm rupture, which include aortic wall injury, inflammatory cell recruitment, and imbalance between elastin and collagen turnover.[14,15,33] Our study was underpowered because only 7 events occurred during follow-up. Further, because most patients were close to having an intervention, they did not have a longer follow-up that would have increased longitudinal testing and more correlations among the tests and the event rate. Despite this, there was a poorer 30-month clinical outcome prediction for patients with aneurysms with increased ^{18}F-FDG PET uptake. This suggests that yearly ^{18}F-FDG PET examination may be a reliable diameter-independent tool for clinical decision making in aortic aneurysms. Unfortunately, a similar dichotomization of FES based on an empirical value was not possible because of the heterogeneity of the study group. Nevertheless, the

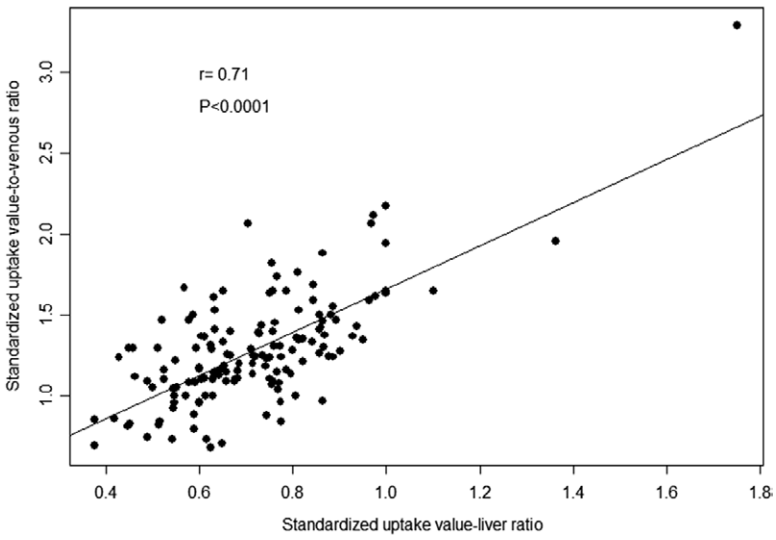

Figure 5. Scatter plot showing a significant positive correlation between quantitative ^{18}F-fluoro-deoxy-glucose uptake, normalized by the liver and the venous background in all patients.

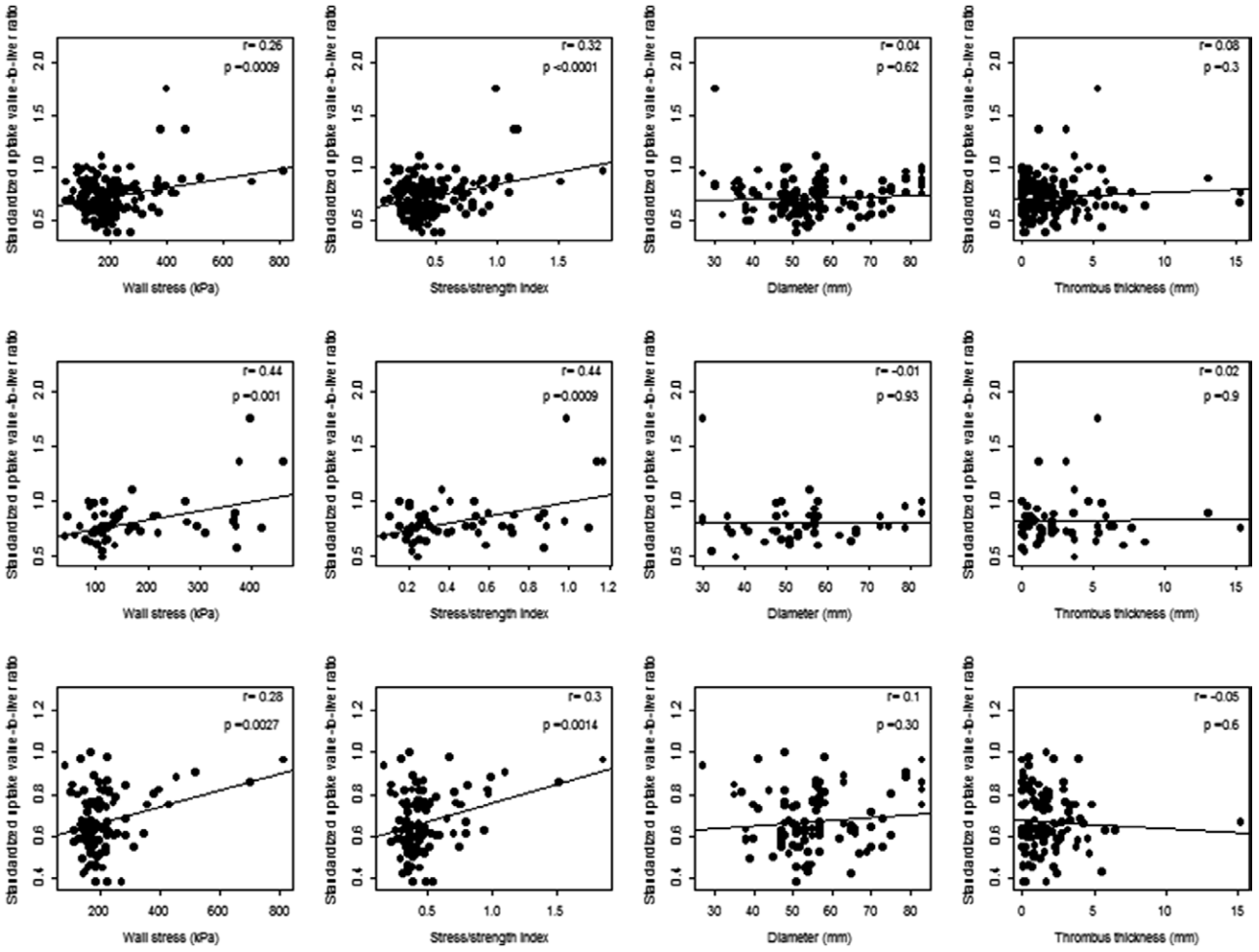

Figure 6. Scatter plots of standardized uptake value-to-liver ratio (SUV_{RL}) vs (from left to right rows) wall stress, wall stress/strength index, maximal diameter, and local thrombus thickness, respectively, for the whole areas (top line), those selected on ^{18}F-fluoro-deoxy-glucose positron emission tomographic imaging (middle line), and those selected on finite element simulation (bottom line). In all groups, a positive correlation is found between SUV_{RL} and both wall stress and wall stress/strength index estimates. No other variable is significantly correlated to SUV_{RL}.

correlation levels between ^{18}F-FDG PET uptake and FES estimates indicate that similar outcome predictions could be expected from qualitative FES.

FES and ^{18}F-FDG PET imaging are fully quantifiable methods. However, evaluating their correlation is technically challenging, mainly because the effect of partial volume and vessel background signaling on both modalities is different. Using a semiquantitative selection of areas of interest, we found modest positive linear relationships between ^{18}F-FDG uptake and FES estimates (correlation range, 0.28–0.44). Our study is the first reporting FES geometry reconstruction without user interaction, obviously resulting in imprecision. We have also identified several determinants for these correlations, including technical factors that can affect the analysis. The correlations with FES parameters were better using a liver rather than a venous-to-background correction, despite a strong correlation between both normalizers. Further, PET scanners have a finite spatial resolution of 5 to 8 mm, causing a low sensitivity to small focus of ^{18}F-FDG uptake, which may account for the mean number of area selection in each examination being lower based on ^{18}F-FDG PET than on FES (1.46±0.69 versus 1.85±0.85 areas per patient).

Angina pectoris and familial aneurysms had a significant effect on the relationship between ^{18}F-FDG uptake and FES estimates.[34] Previously, Verloes et al[35] found that the likelihood of aortic aneurysm rupture is strongly linked to the family history and gene susceptibility. These observations may be related to an alteration in the aortic wall response to stress. Other factors, beyond the scope of the present study, may theoretically influence the relationship between ^{18}F-FDG uptake and wall stress estimates. Wall stress elevation does not necessarily imply increased ^{18}F-FDG uptake. This is illustrated by the fact that in normal and dilated aortas, the magnitude of blood flow velocity decreases gradually from proximal to distal, whereas ^{18}F-FDG uptake does not change in the same magnitude.[19] Finally, it has been reported that an inflammatory reaction related to nonspecific injuries, such as thrombus apposition and calcifications, may result in increased ^{18}F-FDG uptake without wall stress increase.[36]

Study Limitations

The current study has several limitations. Heterogeneity in aneurysm size introduced a potential bias by the lack of previous evidence that both ^{18}F-FDG uptake and wall stress profiles

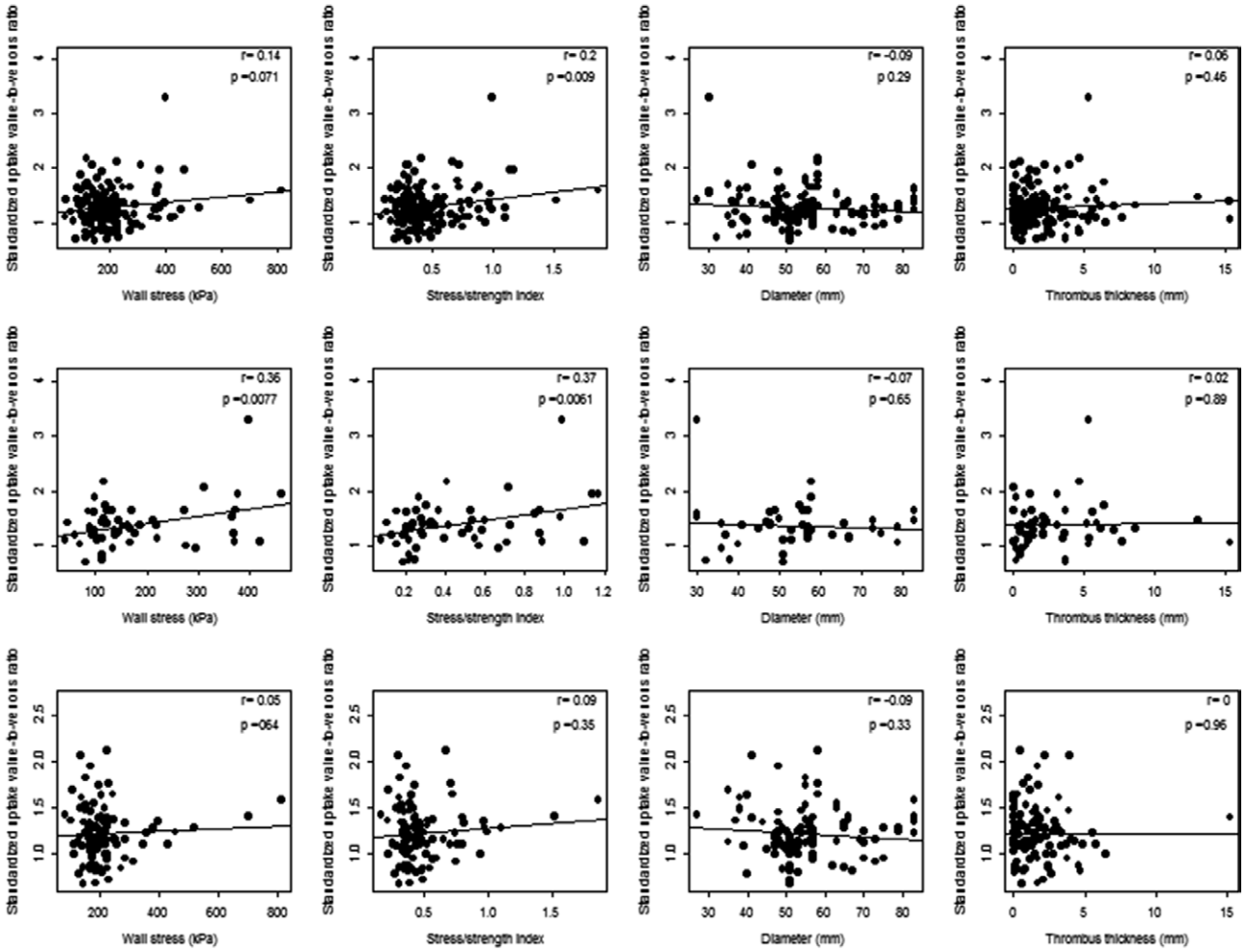

Figure 7. Scatter plots of standardized uptake value-to-venous ratio (SUV_{RV}) vs (from left to right rows) wall stress, wall stress/strength index, maximal diameter, and local thrombus thickness, respectively, for the whole areas (top line), those selected on ^{18}F-fluoro-deoxy-glucose (^{18}F-FDG) positron emission tomographic (PET) imaging (middle line), and those selected on finite element simulation (bottom line). In all areas, a positive correlation is found between SUV_{RV} and wall stress and stress/strength index estimate. In ^{18}FDG PET selected areas, a positive correlation is found between SUV_{RV} and both wall stress and wall stress/strength index estimates. No other variable is significantly correlated to SUV_{RV}.

are similar in small and large aneurysms. AAAs largely outnumbered TAAs, although this reflects their relative proportions in the general population. It obviously resulted in comparison bias between aortic aneurysm types. This study was designed for a time point correlation between variables obtained from a single examination. The fact that most of the AAAs and TAAs were, respectively, >50 and >55 mm in diameter did not allow sufficient follow-up data because most patients were readily eligible for repair. Further, ^{18}F-FDG activity may change over time, whereas wall stress is unlikely to change in the same manner. However, these changes over time have never been studied. This was difficult in our study because of limited follow-up examinations dictated by the time scale and entry-point heterogeneities. The isotropic model, which assumes that wall stress is the same in all directions, has been used here because it is easier to estimate, whereas an anisotropic model would have been more realistic and would allow for more accurate correlations. As in other studies, wall thickness assumption was independent of the underlying intraluminal thrombus. Although both are strongly related,[30] there is no valid way to measure the wall thickness (therefore, inappropriately the same wall thickness is used throughout the aneurysm) of aneurysmal aorta containing intraluminal thrombus and atherosclerotic changes. Despite all these assumptions, the FES model used in the present study has been validated in the sense that it retrospectively discriminated ruptured and intact AAAs.[37]

Finally, low wall shear stress because of blood flow might also be related to metabolic activity by inducing inflammatory responses.[38] Nevertheless, wall shear stress predictions would have required computational fluid dynamics simulations, which are known to be sensitive to inflow conditions (ie, aortic blood flow velocity at the level of the renal arteries), that were unfortunately not available.

Conclusions

^{18}F-FDG uptake and estimates of wall stress and stress/strength index, using the data from a single examination, showed better positive correlations in TAAs than in AAAs. The signaling relationships are related to the properties of both imaging techniques and become more complex by the influence of patient-specific risk factors such as inherited susceptibilities. The findings of this study warrant further investigations

Table 3. Evaluation of SUV_{RV} as a Function of Area Selection Method, Imaging and FES Parameters, and Subjects' Risk Factors (n=163)

Variable	Regression Coefficient±SE	*P* Value*
Area selection technique (FES)	−0.04±0.071	0.57
Maximal aortic diameter	−0.004±0.004	0.26
Wall stress, kPa	0.0010±0.002	0.54
Wall stress/strength	−0.48±0.62	0.43
Local diameter	0.0007±0.003	0.83
Thrombus thickness	0.024±0.016	0.15
Aneurysm location (AAA)	−0.30±0.13	0.027
Age	0.006±0.005	0.29
Sex (male)	−0.060±0.12	0.63
Current smoking	−0.15±0.10	0.15
Stopped smoking	−0.19±0.10	0.061
COPD	−0.11±0.078	0.17
Stroke	−0.062±0.092	0.51
Peripheral artery disease	−0.029±0.077	0.71
Angina pectoris	0.23±0.087	0.012
Renal insufficiency	−0.12±0.095	0.20
Acute myocardial infarction	−0.069±0.078	0.38
Familial aneurysm	0.37±0.13	0.0065

AAA indicates abdominal aortic aneurysm; COPD, chronic obstructive pulmonary disease; ^{18}F-FDG, ^{18}F-fluoro-deoxy-glucose; FES, finite element simulation; PET, positron emission tomography; and SUV_{RV}, standardized uptake value-to-venous background.

*Adjusted for repeated values.

in larger trials with prospective long-term data to identify patients at risk for clinical events and to better determine the relationships among wall biomechanics, blood flow interaction, wall remodeling, and inflammation.

Acknowledgments

We thank Cécile Wégria and Isabelle Mancini for article handling, editing, and management; Martin Auer for A4clinics software support; and Roland Hustinx, MD, PhD, for technical advice in ^{18}F-fluoro-deoxy-glucose positron emission tomography imaging data interpretation.

Sources of Funding

The study was supported by the European Union Seventh Framework Programme (FP7) Fighting Aneurysmal Diseases No. 200647[25] and a grant of impulsion from University of Liège.

Disclosures

None.

References

1. Gillum RF. Epidemiology of aortic aneurysm in the United States. *J Clin Epidemiol*. 1995;48:1289–1298.
2. Bengtsson H, Sonesson B, Bergqvist D. Incidence and prevalence of abdominal aortic aneurysms, estimated by necropsy studies and population screening by ultrasound. *Ann N Y Acad Sci*. 1996;800:1–24.
3. Dillavou ED, Muluk SC, Makaroun MS. Improving aneurysm-related outcomes: nationwide benefits of endovascular repair. *J Vasc Surg*. 2006;43:446–451; discussion 451.
4. Greenhalgh RM, Brown LC, Powell JT, Thompson SG, Epstein D, Sculpher MJ; United Kingdom EVAR Trial Investigators. Endovascular versus open repair of abdominal aortic aneurysm. *N Engl J Med*. 2010;362:1863–1871.
5. Brady AR, Thompson SG, Fowkes FG, Greenhalgh RM, Powell JT; UK Small Aneurysm Trial Participants. Abdominal aortic aneurysm expansion: risk factors and time intervals for surveillance. *Circulation*. 2004;110:16–21.
6. Elefteriades JA. Natural history of thoracic aortic aneurysms: indications for surgery, and surgical versus nonsurgical risks. *Ann Thorac Surg*. 2002;74:S1877–S1880; discussion S1892.
7. Brewster DC, Cronenwett JL, Hallett JW Jr, Johnston KW, Krupski WC, Matsumura JS; Joint Council of the American Association for Vascular Surgery and Society for Vascular Surgery. Guidelines for the treatment of abdominal aortic aneurysms. Report of a subcommittee of the Joint Council of the American Association for Vascular Surgery and Society for Vascular Surgery. *J Vasc Surg*. 2003;37:1106–1117.
8. Darling RC, Messina CR, Brewster DC, Ottinger LW. Autopsy study of unoperated abdominal aortic aneurysms. The case for early resection. *Circulation*. 1977;56(3 Suppl):II161–II164.
9. Nicholls SC, Gardner JB, Meissner MH, Johansen HK. Rupture in small abdominal aortic aneurysms. *J Vasc Surg*. 1998;28:884–888.
10. Brown LC, Powell JT. Risk factors for aneurysm rupture in patients kept under ultrasound surveillance. UK Small Aneurysm Trial Participants. *Ann Surg*. 1999;230:289–296; discussion 296.
11. Zienkiewicz OC, Taylor R.L., J.Z. Zhu. *The Finite Elements Method. The Basis*. 5th ed. Oxford, United Kingdom: Butterworth-Heinemann; 2000.
12. Raghavan ML, Hanaoka MM, Kratzberg JA, de Lourdes Higuchi M, da Silva ES. Biomechanical failure properties and microstructural content of ruptured and unruptured abdominal aortic aneurysms. *J Biomech*. 2011;44:2501–2507.
13. Gasser TC, Görgülü G, Folkesson M, Swedenborg J. Failure properties of intraluminal thrombus in abdominal aortic aneurysm under static and pulsating mechanical loads. *J Vasc Surg*. 2008;48:179–188.
14. Michel JB, Thaunat O, Houard X, Meilhac O, Caligiuri G, Nicoletti A. Topological determinants and consequences of adventitial responses to arterial wall injury. *Arterioscler Thromb Vasc Biol*. 2007;27:1259–1268.
15. Fontaine V, Jacob MP, Houard X, Rossignol P, Plissonnier D, Angles-Cano E, Michel JB. Involvement of the mural thrombus as a site of protease release and activation in human aortic aneurysms. *Am J Pathol*. 2002;161:1701–1710.
16. Houard X, Rouzet F, Touat Z, Philippe M, Dominguez M, Fontaine V, Sarda-Mantel L, Meulemans A, Le Guludec D, Meilhac O, Michel JB. Topology of the fibrinolytic system within the mural thrombus of human abdominal aortic aneurysms. *J Pathol*. 2007;212:20–28.
17. Defawe OD, Colige A, Lambert CA, Munaut C, Delvenne P, Lapière CM, Limet R, Nusgens BV, Sakalihasan N. TIMP-2 and PAI-1 mRNA levels are lower in aneurysmal as compared to athero-occlusive abdominal aortas. *Cardiovasc Res*. 2003;60:205–213.
18. Sakalihasan N, Michel JB. Functional imaging of atherosclerosis to advance vascular biology. *Eur J Vasc Endovasc Surg*. 2009;37:728–734.
19. Truijers M, Kurvers HA, Bredie SJ, Oyen WJ, Blankensteijn JD. *In vivo* imaging of abdominal aortic aneurysms: increased FDG uptake suggests inflammation in the aneurysm wall. *J Endovasc Ther*. 2008;15:462–467.
20. Kotze CW, Menezes LJ, Endozo R, Groves AM, Ell PJ, Yusuf SW. Increased metabolic activity in abdominal aortic aneurysm detected by 18F-fluorodeoxyglucose (18F-FDG) positron emission tomography/computed tomography (PET/CT). *Eur J Vasc Endovasc Surg*. 2009;38:93–99.
21. Sakalihasan N, Hustinx R, Limet R. Contribution of PET scanning to the evaluation of abdominal aortic aneurysm. *Semin Vasc Surg*. 2004;17:144–153.
22. Defawe OD, Hustinx R, Defraigne JO, Limet R, Sakalihasan N. Distribution of F-18 fluorodeoxyglucose (F-18 FDG) in abdominal aortic aneurysm: high accumulation in macrophages seen on PET imaging and immunohistology. *Clin Nucl Med*. 2005;30:340–341.
23. Reeps C, Essler M, Pelisek J, Seidl S, Eckstein HH, Krause BJ. Increased 18F-fluorodeoxyglucose uptake in abdominal aortic aneurysms in positron emission/computed tomography is associated with inflammation, aortic wall instability, and acute symptoms. *J Vasc Surg*. 2008;48:417–423; discussion 424.
24. Xu XY, Borghi A, Nchimi A, Leung J, Gomez P, Cheng Z, Defraigne JO, Sakalihasan N. High levels of 18F-FDG uptake in aortic aneurysm wall are associated with high wall stress. *Eur J Vasc Endovasc Surg*. 2010;39:295–301.
25. http://ec.europa.eu/research/health/medical-research/cardiovascular-diseases/projects/fad_en.html. Accessed November 25, 2013.

26. *A4clinics User Manual vers. 3.0 VG*. A4clinics, Vascops GmbH, Graz, Austria.
27. Reeps C, Gee MW, Maier A, Pelisek J, Gurdan M, Wall W, Mariss J, Eckstein HH, Essler M. Glucose metabolism in the vessel wall correlates with mechanical instability and inflammatory changes in a patient with a growing aneurysm of the abdominal aorta. *Circ Cardiovasc Imaging*. 2009;2:507–509.
28. Maier A, Gee MW, Reeps C, Eckstein HH, Wall WA. Impact of calcifications on patient-specific wall stress analysis of abdominal aortic aneurysms. *Biomech Model Mechanobiol*. 2010;9:511–521.
29. Wang DH, Makaroun MS, Webster MW, Vorp DA. Effect of intraluminal thrombus on wall stress in patient-specific models of abdominal aortic aneurysm. *J Vasc Surg*. 2002;36:598–604.
30. Kazi M, Thyberg J, Religa P, Roy J, Eriksson P, Hedin U, Swedenborg J. Influence of intraluminal thrombus on structural and cellular composition of abdominal aortic aneurysm wall. *J Vasc Surg*. 2003;38:1283–1292.
31. Dobrin PB. Pathophysiology and pathogenesis of aortic aneurysms. Current concepts. *Surg Clin North Am*. 1989;69:687–703.
32. Fillinger MF, Marra SP, Raghavan ML, Kennedy FE. Prediction of rupture risk in abdominal aortic aneurysm during observation: wall stress versus diameter. *J Vasc Surg*. 2003;37:724–732.
33. Sakalihasan N, Limet R, Defawe OD. Abdominal aortic aneurysm. *Lancet*. 2005;365:1577–1589.
34. Nordon IM, Hinchliffe RJ, Loftus IM, Thompson MM. Pathophysiology and epidemiology of abdominal aortic aneurysms. *Nat Rev Cardiol*. 2011;8:92–102.
35. Verloes A, Sakalihasan N, Koulischer L, Limet R. Aneurysms of the abdominal aorta: familial and genetic aspects in three hundred thirteen pedigrees. *J Vasc Surg*. 1995;21:646–655.
36. Georgakarakos E, Ioannou CV, Papaharilaou Y, Kostas T, Tsetis D, Katsamouris AN. Peak wall stress does not necessarily predict the location of rupture in abdominal aortic aneurysms. *Eur J Vasc Endovasc Surg*. 2010;39:302–304.
37. Gasser TC, Auer M, Labruto F, Swedenborg J, Roy J. Biomechanical rupture risk assessment of abdominal aortic aneurysms: model complexity versus predictability of finite element simulations. *Eur J Vasc Endovasc Surg*. 2010;40:176–185.
38. Cecchi E, Giglioli C, Valente S, Lazzeri C, Gensini GF, Abbate R, Mannini L. Role of hemodynamic shear stress in cardiovascular disease. *Atherosclerosis*. 2011;214:249–256.

CLINICAL PERSPECTIVE

The maximal diameter remains the only validated criterion for preventive repair in asymptomatic aortic aneurysm. Because aortic aneurysm is an aging disease, the operative risk has to account for comorbidities that often make clinical decisions difficult. We compared 2 alternative approaches to assess the clinical risk associated with aortic aneurysm using ^{18}F fluoro-deoxyglucose positron emission tomography and finite element simulations. Our study revealed that increased fluoro-deoxy-glucose uptake in aortic aneurysm was associated with a higher risk of clinical event. Provided this finding is replicated in larger series, fluoro-deoxy-glucose uptake could serve as an additional independent factor in the management of patients with aortic aneurysms. Fluoro-deoxy-glucose uptake and wall stress were positively correlated and were both higher in thoracic than in abdominal aortic aneurysms. The strength of association, however, may strongly depend on technical and patient-specific factors, probably related to the ability of the aneurysmal wall to respond appropriately to wall stress.

SUPPLEMENTAL MATERIAL

Supplementary method 1

^{18}F-FDG PET CT imaging

All patients underwent the same image acquisition protocol. After a minimum of 6h fasting, 3.7 MBq ^{18}F-FDG/Kg body weight (mean activity/patient: 277 MBq, range: 202-394 MBq) was injected through a peripheral vein catheter. The patient was placed into a quiet room and instructed not to move. All patients had glucose serum levels below the threshold of 200 mg/dl, except one (292 mg/dl). Approximately 1h (mean: 69 min, range: 54-100 min) after injection of ^{18}F-FDG, static whole-body examination was performed with a PET-CT scanner Discovery LS (General Electrics Healthcare, Milwaukee, WI). The CT component of this scanner (LightSpeed Ultra) can acquire 4 slices per X-ray tube rotation.

After scout views, CT was performed from the skull base to the femoral necks 50 seconds after the start of intravenous injection of 120 ml of an iodinated contrast agent (Omnipaque 350 mg of I/ml, General Electrics Healthcare, Diegem, Belgium) into an antecubital vein, at a rate of 2 ml/s. CT parameters were: 5 mm collimation, 50 x 50 cm field-of-view (FOV), 120 kVp, pitch of 1.5:1, gantry rotation cycle of 0.8 s, and automatic adaptation of the amperage at each tube rotation, optimized with indications provided by the scout views. During CT data acquisition, the patients were asked to hold breath at an average lung volume as long as they can, and if necessary, to breath shallowly until the end of acquisition. Thereafter, emission images were recorded at each bed position for 4 minutes. PET raw data were reconstructed as coronal 4.25 mm slice-thickness overlapping from 15-30%, by mean of ordered subset expectation maximization (OSEM) reconstruction algorithm

performed with 2 iterations and 21 ordered subsets (pixel matrix of 128 x 128 and FOV of 50 cm), with 5.86 mm full width at mid-height (FWHM) post filter and 3.91 mm FWHM loop filter, model-based scatter correction (convolution subtraction) and normalization correction. To decrease the total radiation dose, PET data attenuation correction was performed using contrast-enhanced CT raw data that cause a 20-40% overcorrection [1-3].

FES

Aneurysms were reconstructed off-line from the CT images by an experienced operator blinded to patient and ^{18}F-FDG PET data, with the diagnostic system *A4clinics* (VASCOPS GmbH, Graz, Austria)[4]. The reconstruction was based on deformable models [5], which require minimal user interactions and provide operator insensitive results [6]. The finite element method [7] is an established numerical concept that divides any geometry into a large number of small finite elements, which together define a structural model of the aneurysm including a hypothetical wall-thrombus limit paralleling the external aortic contour (Figure 1). The hypothetical finite element model is pressurized by the mean arterial pressure (1/3 systolic pressure + 2/3 diastolic pressure). The applied models considered isotropic constitutive descriptions for the intraluminal thrombus [8] and the aneurysm wall [9] . An isotropic constitutive model is thought to be an acceptable approximation and assumes that the tissue's mechanical properties do not depend on the orientation, i.e. the stress-strain responses of circumferential and longitudinal strips of tissue are identical. In this study, the same wall thickness assumptions were applied to TAAs and AAAs. Finite element models used in this study specifically adjust the wall thickness inversely proportional to the amount of intraluminal thrombus[10], as this is required for accurate

stress predictions [11]. Further details regarding the concept and assumptions used by *A4clinics* are given elsewhere [4, 5].

For each aneurysm, the detailed FES predicted the distribution of the wall stress all over the aorta. Specifically, the von Mises stress $\sigma_M = \{[(\sigma_1 - \sigma_2)^2 + \sigma_1^2 + \sigma_2^2]/2\}^{0.5}$ was used to represent the biaxial stress state by a single stress value. Here, σ_1 and σ_2 denote respectively the principal stress components, i.e. the circumferential and axial stresses in the wall. Relating this stress to estimated wall strength defines a stress/strength index. The used wall strength model was based on in-vitro failure tests of AAA wall samples [12]. The applied model considered heterogeneous wall strength that accounted for local wall weakening influenced by the ILT, gender, family history and the ratio between the local diameter and the normal infrarenal aortic diameter [12].

Supplementary method 2

Relative intensity of a Finite Element Simulation (FES) estimate = [(recorded maximal value – mean value of the whole aorta)/(maximal value of the whole aorta – mean value of the whole aorta)] x100.

Supplementary method 3

^{18}F-FDG Standardized Uptake Value (SUV) allows inter-subject comparisons by removing most of the differences due to body weight and injected dose, using the following formula:

SUV = [^{18}F-FDG uptake (MBq/g) x patient weight (g)] / injected activity (MBq).

Supplementary table1: Detailed clinical outcomes after the first examination

	Unoperated		Operated	Other causes of follow-up termination	
	Uneventful follow-up	Death from unrelated cause	Oversized	Growth (> 1cm/year)	Acute rupture/dissection
Patients (n = 53)	24	7 (2)	15 (1)	4	(3) (3)
Follow-up duration (months)	15.4±6.6	9.3±8.0	5.7±8.5	10.8±11.8	6.0±4.6
Initial aneurysm diameter (mm)	41.7±6.5	47.8±8.5	56,5±9.4	48.4±5.5	65.3±12.9
PET-(n = 35)	19	5 (1)	9	2	0
PET+(n = 18)	5	2 (1)	6 (1)	2	3
FES Co-localization	*2*	*1 (1)*	*0*	*0*	*1*

Terminated follow-up are on gray background and significant clinical events right to the vertical line.

Between parentheses are the patients with TAAs.

PET = Positron Emission Tomography, ^{18}F-FDG = 18-fluoro-deoxy-glucose, FES = Finite Element Simulation.

PET+ are patients with aortic area of ^{18}F-FDG uptake on PET images, and PET- refers to no uptake.

FES co-localization (in italics) refers to the subgroup of PET+ patients in areas co-localized with a maximal value of a FES estimate.

References

1. A4clinics User Manual vers. 3.0 VG.
2. Mawlawi O, Erasmus JJ, Pan T, Cody DD, Campbell R, Lonn AH, Kohlmyer S, Macapinlac HA, Podoloff DA. Truncation artifact on pet/ct: Impact on measurements of activity concentration and assessment of a correction algorithm. *AJR. American journal of roentgenology*. 2006;186:1458-1467
3. Vera P, Ouvrier MJ, Hapdey S, Thillays M, Pesquet AS, Diologent B, Callonec F, Hitzel A, Edet-Sanson A, Menard JF, Jardin F, Tilly H. Does chemotherapy influence the quantification of suv when contrast-enhanced ct is used in pet/ct in lymphoma? *European journal of nuclear medicine and molecular imaging*. 2007;34:1943-1952
4. Kotze CW, Groves AM, Menezes LJ, Harvey R, Endozo R, Kayani IA, Ell PJ, Yusuf SW. What is the relationship between (1)(8)f-fdg aortic aneurysm uptake on pet/ct and future growth rate? *European journal of nuclear medicine and molecular imaging*. 2011;38:1493-1499
5. Auer M, Gasser TC. Reconstruction and finite element mesh generation of abdominal aortic aneurysms from computerized tomography angiography data with minimal user interactions. *IEEE transactions on medical imaging*. 2010;29:1022-1028
6. Hyhlik-Durr A, Krieger T, Geisbusch P, Kotelis D, Able T, Bockler D. Reproducibility of deriving parameters of aaa rupture risk from patient-specific 3d finite element models. *Journal of endovascular therapy : an official journal of the International Society of Endovascular Specialists*. 2011;18:289-298
7. Zienkiewicz OC TR e. The finite elements method. The basis. 5th edition ed. Oxford:Butterworth heinemann; n°1. 2000

8. Gasser TC, Gorgulu G, Folkesson M, Swedenborg J. Failure properties of intraluminal thrombus in abdominal aortic aneurysm under static and pulsating mechanical loads. *Journal of vascular surgery*. 2008;48:179-188

9. Raghavan ML, Vorp DA. Toward a biomechanical tool to evaluate rupture potential of abdominal aortic aneurysm: Identification of a finite strain constitutive model and evaluation of its applicability. *Journal of biomechanics*. 2000;33:475-482

10. Kazi M, Thyberg J, Religa P, Roy J, Eriksson P, Hedin U, Swedenborg J. Influence of intraluminal thrombus on structural and cellular composition of abdominal aortic aneurysm wall. *Journal of vascular surgery*. 2003;38:1283-1292

11. Gasser TC, Auer M, Labruto F, Swedenborg J, Roy J. Biomechanical rupture risk assessment of abdominal aortic aneurysms: Model complexity versus predictability of finite element simulations. *European journal of vascular and endovascular surgery : the official journal of the European Society for Vascular Surgery*. 2010;40:176-185

12. Vande Geest JP, Wang DH, Wisniewski SR, Makaroun MS, Vorp DA. Towards a noninvasive method for determination of patient-specific wall strength distribution in abdominal aortic aneurysms. *Annals of biomedical engineering*. 2006;34:1098-1106